Proceedings of the Canadian Society for Mechanical Engineering International Congress
32nd Annual Conference of the Computational Fluid Dynamics Society of Canada
Canadian Society of Rheology Symposium
CSME-CFDSC-CSR 2025
May 25–28, 2025, Montréal, Québec, Canada

Effect of Frosting on Performance and Greenhouse Gas Emissions of Absorption Heat Pumps in Cold Climates

Tahmid Ibn Sayeed [1], Siddhartha Gollamudi [1], Melanie Fauchoux [1], Samira Payan[1,2], Carey Simonson[1]
[1] Department of Mechanical Engineering, University of Saskatchewan, Saskatoon, Canada
[2]Department of Mechanical Engineering, University of Sistan and Baluchestan, Zahedan, Iran
qpt349@usask.ca

Abstract—Air source heat pumps can be used as an alternative to natural gas furnaces in efforts to reduce annual heating energy consumption and greenhouse gas emissions. However, in cold climates, the performance of air source heat pumps can be affected by frost formation on the evaporator surface. The performance reduction will in turn lead to an increase in energy consumption and greenhouse gas emissions. This paper aims to quantify the effect of frosting on the performance, energy consumption and greenhouse gas emissions of natural gas driven air source heat pumps called gas absorption heat pumps (GAHPs) in eight different Canadian cities.

GAHPs experienced between 1%-2% increase in energy consumption due to frosting across the 8 different Canadian cities. In comparison, electric air source heat pumps (ASHPs) may experience up to 20% increase in energy consumption. Therefore, GAHPs could be a potential replacement for natural gas furnace heating, over ASHPs, in cold climates (where frosting is a prevalent problem).

Keywords- Gas absorption heat pump; Natural gas heat pump; Space heating; Cold climate heat pump; Frosting; Building decarbonization

I. INTRODUCTION

Buildings are responsible for 40% of the total energy consumption and 13% of the total greenhouse gas (GHG) emissions in developed countries such as Canada [1], [2]. Building heating systems are the primary cause of this high energy consumption and GHG emissions in buildings. Natural gas furnaces are typically used to provide space heating in many parts of Canada. Replacing natural gas furnaces with air source heat pumps can significantly reduce GHG emissions and annual heating energy consumption. Air source heat pumps use heat from the ambient air to heat the building and typically have COPs greater than 1.

When air is used as the heat source, one component of the heat pump, the evaporator, is located outdoors. In cold climates, frosting occurs when moisture in the air freezes on the evaporator surface. Water condenses when the surface temperature of the evaporator is lower than the dew-point temperature of the air. If the temperature of the evaporator surface is also below 0℃ then the condensate will solidify and form frost [3]. Frost can also form directly by desublimation [4]. The formation of frost can negatively impact the performance of a heat pump. If the frost is not melted off the evaporator surface, it might also lead to physical damage to the heat pump unit [5]. Therefore, a frosted evaporator must be defrosted regularly, to ensure proper operation of the heat pump.

There are two types of air source heat pumps, classified by their working principle: electric air source heat pumps (ASHP) and gas absorption heat pumps (GAHP). Previous researchers have reported electric ASHPs experiencing significant performance reduction and an increase in energy consumption due to frosting/defrosting operations. Rossi et al. [6] reported up to 9% reduction in the seasonal coefficient of performance (SCOP) of ASHPs in Italy. Shao et al. [7] calculated a 32% reduction in the hourly coefficient of performance (COP) due to frosting. Wei et al. [8] reported that frosting caused an increase in energy consumption of up to 17.4% and a decrease in SCOP by 14.8% in China. Gollamudi et al. [3] reported up to 20% increase in annual energy consumption in Saskatoon, Canada.

In general, electric ASHPs have higher COPs than GAHPs. However when the ambient air temperatures are lower, the difference between the COP of an electric ASHP and a GAHP decreases [9], [10]. This diminishing gain in performance coupled with the 3-6 times lower natural gas prices compared to electricity seen in Canada, can make GAHPs, a more practical replacement for natural gas furnace heating in cold climates [11], [12]. Additionally in cities like Saskatoon, GAHPs could also potentially have lower GHG emissions due to the higher emission intensity of the electricity grid in

Saskatchewan compared to the emission intensity of generating energy from natural gas [13], [14].

While many researchers have studied the effect of frosting on electric ASHPs, very few studies exist on frosting in GAHPs. This paper will quantify the effect of frosting on the performance of GAHPs in cold climates. Simulations were performed for eight different cities across Canada. These cities, each have different climates, but are all still considered cold climates, with heating required for a portion of the year. The heating design temperature, ASHRAE climate zone and the heating degree days for each city are shown in Table 1.

Table 1: ASHRAE heating design temperature, heating degree days and ASHRAE climate zones for the Canadian cities considered in this paper [15].

City	***Province***	***Design temperature*** [℃]	***Heating degree days***	***Climate zone***
Saskatoon	SK	−30.7	5853	7
Winnipeg	MB	−29.6	5697	7
Calgary	AB	−24.5	5054	7
Fredericton	NS	−20.3	4541	6
Charlottetown	PEI	−17.1	4511	6
Montreal	QC	−20.2	4257	6
Toronto	ON	−15.7	3779	5
Vancouver	BC	−3.0	2873	4

II. METHODOLOGY

A. *Building energy simulation*

A small office building was modelled based on the United States Department of Energy (DOE) benchmark models for commercial buildings [16]. Building energy simulations were performed using eQuest [17] to determine the hourly heating load of the building. The single-story office building has one core zone and four perimeter zones. The overall heat transfer coefficients of the building envelope are specified in Table 2. The floor area, design ventilation, design maximum occupancy and infiltration rate can be found in Table 3.

Table 2: Overall heat transfer coefficients for the walls, roof and windows [16].

Location	***U-Value*** $\left(\frac{W}{m^2K}\right)$
Wall	0.51
Roof	0.15
Window	2.62

Table 3: Floor Space, Design Ventilation, Design Maximum Occupancy and Infiltration of the Building [16].

Parameter	***Value***
Floor space	511 m^2
Design Ventialtion	10 $\frac{L}{s.person}$
Infiltration	0.45 ACH
Design maximum occupancy	18.6 $\frac{m^2}{person}$

B. *Thermodynamic model*

A thermodynamic model of the absorption heat pump was developed as a MATLAB script. A water and lithium chloride solution is the most commonly used working pair in absorption heat pumps, where water is the refrigerant, and lithium chloride is the absorbent. However, water freezes below 0℃ so it cannot be used in cold climates as the refrigerant. Therefore, ammonia and water are chosen as the working pair instead [9], where ammonia is the refrigerant, and water is the absorbent. This allows the absorption heat pump to operate at subzero outdoor air temperatures. A schematic of the absorption heat pump is shown in Fig 1.

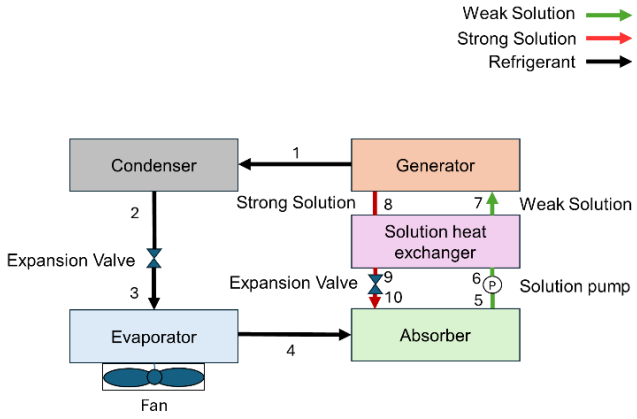

Figure 1: Schematic of an absorption heat pump.

The following assumptions were made in the model [9], [18]:

- Flow resistance, pressure losses and heat losses in the pipes are neglected.
- The solution leaving the generator is pure ammonia.
- The solution pump efficiency is 80%.
- The solution heat exchanger and the evaporator effectiveness are 80%.
- 100 Pa of pressure drop is assumed across the evaporator.
- The efficiency of the fan was assumed to be 70% in this paper.
- Operating temperature for the generator, condenser and absorber was set to 160℃, 50℃ and 40℃ respectively.
- Temperature difference between ambient air and evaporator is 10℃

The enthalpy, pressure, mass fraction, and specific volume of pure ammonia and the ammonia/water mixture were obtained using empirical correlations [19], [20] and Coolprop software [21]. Mass and energy balances across each component were used to obtain the energy transfer rates and mass flowrates through each component [18], [19].

Energy transfer rates for the absorber, condenser, generator and pump can be found using Eqs. (1), (2), (3) and (4), respectively.

$$Q_{abs} = \dot{m}_{ref} h_4 - \dot{m}_{weak} h_5 + \dot{m}_{strong} h_{10} \quad (1)$$

$$Q_{cond} = \dot{m}_{ref}(h_1 - h_2) \quad (2)$$

$$Q_{gen} = \dot{m}_{weak} h_7 - \dot{m}_{strong} h_8 - \dot{m}_{ref} h_1 \quad (3)$$

$$W_{pump} = \dot{m}_{weak}(h_5 - h_6) \quad (4)$$

where $\dot{m}_{ref}\left[\frac{kg}{s}\right]$ is the mass flowrate of the pure refrigerant, $\dot{m}_{weak}\left[\frac{kg}{s}\right]$ is the mass flowrate of the weak solution, $\dot{m}_{strong}\left[\frac{kg}{s}\right]$ is mass flowrate of the strong solution and h $\left[\frac{kJ}{kg}\right]$ is the enthalpy at a specified state point (denoted by the subscripts 1 to 10). The energy consumed by the fan can be calculated using Eq. (5).

$$W_{fan} = \frac{V\Delta P}{\eta_f} \quad (5)$$

where $V\left[\frac{m^3}{s}\right]$ is volumetric flowrate of air, ΔP[Pa] is the pressure change across the fan and η_f is the efficiency of the fan.

The performance of an absorption heat pump is quantified using COP, which can be found using Eq. (6) [22].

$$COP = \frac{Q_{abs} + Q_{cond}}{Q_{gen} + W_{fan} + W_{pump}} = \frac{Q_h}{Q_{gen} + W_{fan} + W_{pump}} \quad (6)$$

where Q_h[kWh] is the heating load of the building obtained using eQuest, Q_{abs}[kWh] is the heat supplied by the absorber, Q_{cond}[kWh] is the heat supplied by the condenser, Q_{gen}[kWh] is the heat supplied to the generator, W_{fan}[kWh] is the energy consumed by the fan and W_{pump}[kWh] is the energy consumed to operate the pump.

The performance of the GAHP over the whole heating season is quantified using the SCOP which can be calculated using Eq. (7) [23].

$$SCOP = \frac{\sum_{i=1}^{N} Q_{h_i}}{\sum_{i=1}^{N} W_i} \quad (7)$$

where Q_{h_i}[kWh] is the heating load from eQuest for hour i, W_i[kWh] is the work done for the hour and *N* is the total number of annual heating hours for a specific city.

Fig. 2 shows the variation in COP of the modeled GAHP and a 95% efficient NG furnace at different ambient temperatures. At temperatures below -31℃ the performance of the absorption heat pump is lower than that of the 95% efficient natural gas furnace. Since lower thermal performance leads to higher energy consumptions, the heating controls in the model are set to ensure minimum energy is consumed annually. If the hourly ambient temperature is below -31℃, the heat pump circuit is bypassed, and space heating is provided by the natural gas furnace mode for that hour. When the hourly temperature increases to -31℃ or more, the GAHP start operating in its regular mode again.

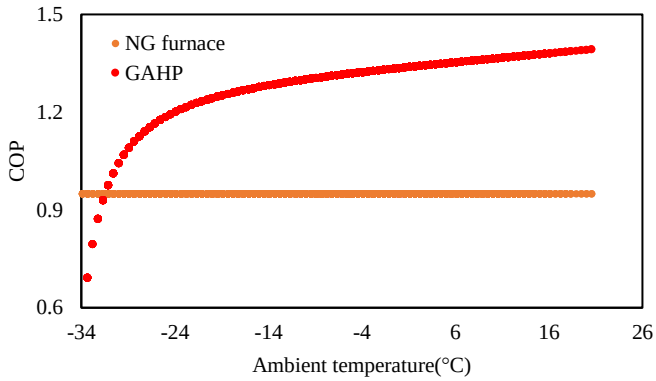

Figure 2: COP/thermal efficiency of a GAHP and NG furnace at different ambient temperatures.

C. *Modelling the effect of frosting on absorption heat pump performance*

Frost formation on the surface of the evaporator can block airflow through the evaporator. This will increase the pressure drop across the evaporator and result in an increase in fan energy consumption. Additionally, heat transfer across the evaporator is also reduced [5]. The increase in fan energy consumption and decrease in heat transfer at the evaporator will negatively impact the COP of the heat pump. Therefore, the frost must be melted from the surface.

Most electric heat pumps use reverse cycle defrosting, in which the heat pump takes heat from the indoor space during the defrost cycle to melt the frost [24]. This will negatively impact the thermal comfort in the indoor spaces. However, absorption heat pumps generally defrost by passing a certain percentage of the hot ammonia vapor (from the outlet of the generator) across the evaporator [24], [25].

At certain outdoor temperatures and relative humidities, typical absorption heat pumps will experience a defrost cycle every 2-3 hours [24]. The defrost cycle typically takes 5 minutes, followed by another 5 minutes of recovery time. This recovery time allows the GAHP to return to its pre-frost performance. It is also important to note that during defrosting operation the GAHPs can still provide heat to the building at a reduced capacity[24], [25]. Therefore, indoor space thermal comfort is not compromised.

Field tests conducted by Sharma et al. [24] showed that GAHPs experience 3-4% reduction in performance due to frosting, depending on the ambient temperature. Table 4 shows frost correction factors (C_f) they determined for the GAHP for each ambient air temperature (T_{amb}) range.

Table 4: Performance correction factors for GAHP due to frosting [24].

Temperature range [℃]	C_f*(%)*
$T_{amb} \geq 3.5$	No performance reduction
$3.5 > T_{amb} \geq -2.7$	4%
$-2.7 > T_{amb} \geq -9$	3%
$T_{amb} < -9$	No performance reduction

It is important to note that only thermal energy from the ammonia vapor is being used for defrosting so the frost-correction factor will directly impact the COP_{gas} instead of the overall COP. COP_{gas} can be calculated using Eq. (8) [26].

$$COP_{gas} = \frac{Q_h}{Q_{gen}} \tag{8}$$

The COP_{gas} can be adjusted using C_f to calculate $COP_{gas(frost)}$ as shown in Eq. (9).

$$COP_{gas(frost)} = COP_{gas} * (1 - C_f) \tag{9}$$

The adjusted $COP_{gas(frost)}$ can then be used to calculate the additional energy required to melt the frost. The additional energy Q_{frost}[kWh] can be calculated using Eq. (10) [10].

$$Q_{frost} = Q_h \left(\frac{1}{COP_{gas(frost)}} - \frac{1}{COP_{gas}} \right) \tag{10}$$

Q_{frost} is then used to calculate the adjusted overall COP of the GAHP, as shown in Eq. (11).

$$COP_{frost} = \frac{Q_h}{Q_{gen} + Q_{frost} + W_{fan} + W_{pump}} \tag{11}$$

D. Adjusting frosting temperature ranges

The temperature difference between the evaporator surface and the ambient air is a key factor that affects frost accumulation at the evaporator [4]. The original model [24],[27] assumes a glide of 2℃ across the evaporator. Considering the glide, the temperature difference between the evaporator and ambient air is between 6℃ and 8℃. However, the thermodynamic model presented in section B uses a 10℃ temperature difference. In order to match the reference paper's temperature difference, the frosting temperature ranges are adjusted, as shown in Table 5. Case 1 represents the adjusted frosting temperature range according to a 6 ℃ temperature difference between the ambient air and the evaporator, and case 2 represents the adjusted frosting temperature range for an 8℃ temperature difference.

Table 5: Adjusted frosting temperature ranges to match the model by Keinath et al [27].

Case 1	*Case 2*	C_f (%)
$T_{amb} \geq 7.5$℃	$T_{amb} \geq 5.5$℃	No performance reduction
7.5℃ $> T_{amb} \geq 1.3$℃	5.5℃ $> T_{amb} \geq -0.7$℃	4%
1.3℃ $> T_{amb} \geq -5$℃	-0.7℃ $> T_{amb} \geq -7$℃	3%
$T_{amb} < -5$℃	$T_{amb} < -7$℃	No performance reduction

E. Energy Consumption and GHG emissions

The energy consumption for the case with no frost is calculated using Eq. (12). The energy consumption considering the frosting/defrosting penalty is calculated using Eq. (13).

$$E_{nf} = \sum_{i=1}^{N} Q_{gen_i} + W_{pump_i} + W_{fan_i} \tag{12}$$

$$E_f = E_{nf} + \sum_{i=1}^{N} Q_{frost_i} \tag{13}$$

An estimate for the annual GHG emissions can be obtained using the GHG emission intensity. Emission intensity is defined as the amount of GHG emissions per kWh of energy produced.

The annual GHG emissions for the no frost and frost cases can be calculated using Eq. (14) and Eq. (15) respectively.

$$e_{nf} = \sum_{i=1}^{N} Q_{gen_i} \dot{e}_{NG} + W_{fan_i} \dot{e}_{EG} + W_{pump_i} \dot{e}_{EG} \tag{14}$$

$$e_f = \sum_{i=1}^{N} Q_{gen_i} \dot{e}_{NG} + W_{fan_i} \dot{e}_{EG} + W_{pump_i} \dot{e}_{EG} + Q_{frost_i} \dot{e}_{NG} \tag{15}$$

where $\dot{e}_{NG}\left[\frac{\text{g of } CO_{2e}}{\text{kWh}}\right]$ is the emission intensity of natural gas and $\dot{e}_{EG}\left[\frac{\text{g of } CO_{2e}}{\text{kWh}}\right]$ is the emission intensity of the electricity grid. Emission intensity of natural gas is considered to be $240\ \frac{\text{g of } CO_{2e}}{\text{kWh}}$ [14]. Whereas Canadian average for electricity grid emission intensity is used as $\dot{e}_{EG}$ (which is $150\ \frac{\text{g of } CO_{2e}}{\text{kWh}}$ [28]).

III. RESULTS AND DISCUSSION

The effect of frosting on the SCOP of GAHP is shown in Fig. 3. Overall, frosting does not affect the SCOP drastically for any of the cities. The maximum difference between the SCOPs when the effect of frosting is considered is 0.029 (or 2.2%).

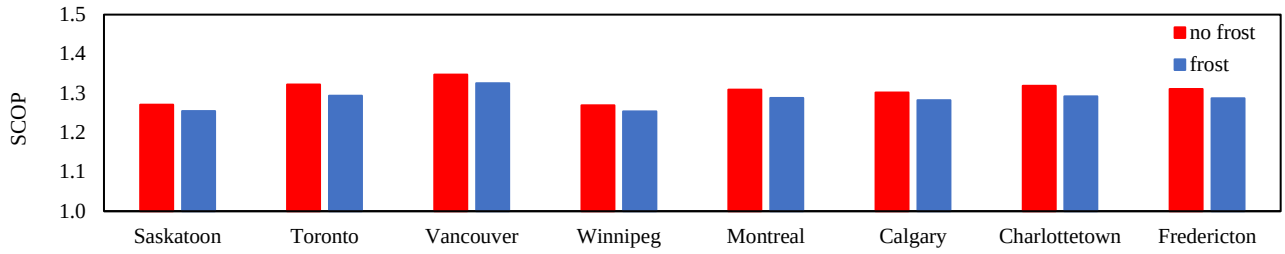

Figure 3: Change in SCOP of GAHPs in Canadian cities due to frosting (using frosting temperature ranges presented in Table 4).

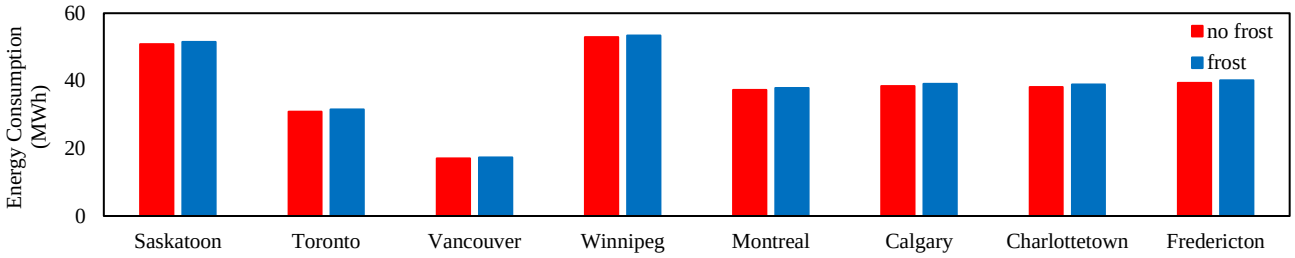

Figure 4: Change in annual energy consumption of GAHPs in Canadian cities due to frosting (using frosting temperature ranges presented in Table 4).

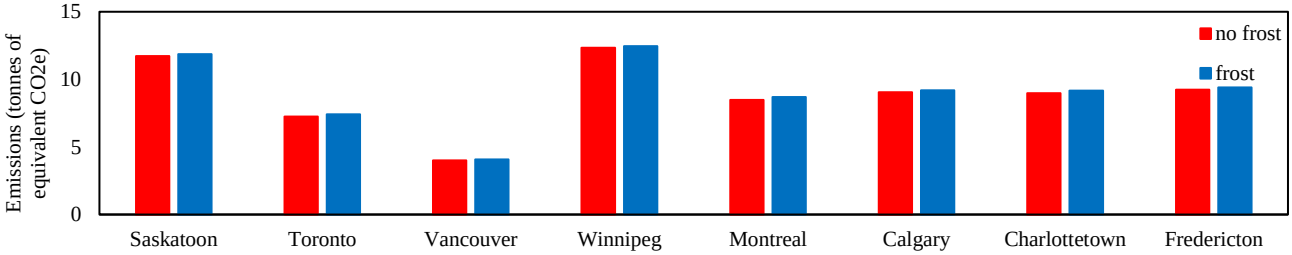

Figure 5: Change in greenhouse gas emissions of GAHPs in Canadian cities due to frosting (using frosting temperature ranges presented in Table 4).

The highest difference was observed in Toronto, whereas the lowest difference was observed in Winnipeg. In Winnipeg, the SCOP only decreases by 0.015 (or 1.2%). The difference in SCOPs of the frost and the no frost cases depend on the percentage of heating hours that each of the cities have in the frosting temperature range of -9℃ to 3.5℃. Winnipeg has about 30% of its heating hours in the frosting temperature range. On the other hand, Toronto has over 57% of its heating hours in the frosting temperature range.

In addition to that about 34% of the Toronto's heating hours are between a temperature range of −2.7℃ and 3.5℃. In comparison to that only 16% of the heating hours in Winnipeg are between −2.7℃ and 3.5℃. In this temperature range (of −2.7℃ and 3.5℃), the performance reduction due to frosting is greater as the amount of moisture in the air is higher compared to lower ambient air temperatures. This leads to faster frost accumulation on the evaporator surface.

Fig.4 and Fig. 5 shows how frosting affects the annual heating energy consumption and GHG emissions in the eight different cities. Due to the decrease in SCOPs, both energy consumption and GHG emissions increase by 1%-2%. Toronto and Winnipeg are the cities which experience the largest and the smallest increase, in energy consumption and GHG emissions, respectively.

Adjusting the temperature range to Case 1 and Case 2, presented in Table 5, showed minimal effect on the SCOP values. The SCOP values only deviated up to 1.1%. Therefore, it was concluded that the frost correction factors in the reference paper can be directly applied to the thermodynamic model discussed in this paper.

Overall, frosting has very minimal impact on the SCOP, energy consumption and GHG emissions of GAHPs.

IV. CONCLUSION

Frosting of the evaporator results in a slight performance reduction in GAHPs. This performance reduction also leads to a slight increase in energy consumption and GHG emissions. However, in comparison to electric ASHPs, the performance reduction is negligible. Previous research has shown that electric ASHPs can experience up to 20% increase in energy consumption. Whereas GAHPs only experience between 1%-2% increase in energy consumption. Therefore, GAHPs can be considered to be virtually frost resistant. In cold climates, where air source heat pumps experience

frosting, GAHPs could potentially be a more suitable alternative to natural gas furnace heating.

ACKNOWLEDGMENT

This research was funded by Natural Sciences and Engineering Research Council of Canada (NSERC).

REFERENCES

[1] L. Pérez-Lombard, J. Ortiz, and C. Pout, "A review on buildings energy consumption information," Energy and Buildings, vol. 40, pp. 394–398, 2008.

[2] Canada Energy Regulator, "Canada Energy Future 2023: Results," Canada energy future. Accessed: Jul. 20, 2024. [Online]. Available: https://www.cer-rec.gc.ca/en/data-analysis/canada-energy-future/2023/results/

[3] S. Gollamudi, E. Krishnan, H. Ramin, G. Annadurai and C. Simonson, "Modelling Air-Source Heat Pumps in Cold Climatic Conditions Considering the Effects of Frosting," Proceedings from uSIM 2022.

[4] R. Tang, F. Wang, Z. Wang, and W. Yang, "Division of Frosting Type and Frosting Degree of the Air Source Heat Pump for Heating in China," Frontiers in Energy Research vol. 9, 2021.

[5] J. Zhu, Y. Sun, W. Wang, Y. Ge, L. Li and J. Liu, "A novel Temperature-Humidity-Time defrosting control method based on a frosting map for air-source heat pumps", International Journal of Refrigeration vol. 54, pp. 45–54, 2015.

[6] E. R. Di Schio, V. Ballerini, M. Dongellini, and P. Valdiserri, "Defrosting of air-source heat pumps: Effect of real temperature data on seasonal energy performance for different locations in Italy," Applied Sciences, vol. 11, 2021.

[7] S. Shao, H. Zhang, X. Fan, S. You, Y. Wang, and S. Wei, "Thermodynamic and economic analysis of the air source heat pump system with direct-condensation radiant heating panel," Energy, vol. 225, 2021.

[8] W. Wei, B. Wang, H. Gu, L. Ni, and Y. Yao, "Investigation on the regulating methods of air source heat pump system used for district heating: Considering the energy loss caused by frosting and on–off," Energy and Building, vol. 235, 2021.

[9] W. Wu, X. Zhang, X. Li, W. Shi, and B. Wang, "Comparisons of different working pairs and cycles on the performance of absorption heat pump for heating and domestic hot water in cold regions," Applied Thermal Engineering, vol. 48, pp. 349–358, 2012.

[10] S. Gollamudi, M. Fauchoux, E. Krishnan, H. Ramin, A. Joseph, and C. Simonson, "Methodology to evaluate design modifications intended to eliminate frosting and high discharge temperatures in air-source heat pumps (ASHPs) in cold climates," Energy and Buildings, vol. 312, 2024.

[11] Energy Hub, "Electricity prices in canada 2023." Accessed: Aug. 14, 2024. [Online]. Available: https://www.energyhub.org/electricity-prices/#:~:text=uniform daily usage.-,Saskatchewan,%24182 per month in 2020.

[12] Canada Energy Regulator, "Market Snapshot: What is in your residential natural gas bill?," Market snapshot. Accessed: Apr. 08, 2024. [Online]. Available: https://www.cer-rec.gc.ca/en/data-analysis/energy-markets/market-snapshots/2018/market-snapshot-what-is-in-your-residential-natural-gas-bill.html

[13] Canada Energy Regulator, "CER- Provincial and Territorial Energy Profiles – Saskatchewan," Provincial and terrirorial energy profiles. Accessed: Jun. 08, 2024. [Online]. Available: https://www.cer-rec.gc.ca/en/data-analysis/energy-markets/provincial-territorial-energy-profiles/provincial-territorial-energy-profiles-saskatchewan.html

[14] City of Regina, "Measuring energy and greenhouse gas." Accessed: Aug. 23, 2024. [Online]. Available: https://www.regina.ca/about-regina/renewable-regina/get-involved-and-learn-more/measuring-energy-greenhouse-gas/

[15] ASHRAE, "ASHRAE CLIMATIC DESIGN CONDITIONS 2009/2013/2017/2021." Accessed: Jan. 22, 2025. [Online]. Available: https://ashrae-meteo.info/v2.0/

[16] P. Torcellini, M. Deru, B. Griffith, and K. Benne, "DOE Commercial Building Benchmark Models Preprint," 2008. [Online]. Available: http://www.nrel.gov/docs/fy08osti/43291.pdf

[17] J. J. Hirsch, "Equest." Accessed: Jul. 22, 2024. [Online]. Available: https://www.doe2.com/equest/#:~:text=eQUEST was designed to allow,art%22 of building performance modeling.

[18] X. Li, W. Wu, X. Zhang, W. Shi, and B. Wang, "Energy saving potential of low temperature hot water system based on air source absorption heat pump," Applied Thermal Engineering, vol. 48, pp. 317–324, 2012.

[19] D. Sun, "Comparison of the performance of NH3-H20, NH3-LiNO3 and NH3-NaSCN absorption refrigeration system," Energy Conversion and Management, vol. 39, pp. 357–368, 1998

[20] P. Waghare and A. Sathyabhama, "Performance analysis of ammonia-based vapour absorption refrigeration system," Materials Today Proceedings, vol. 51, pp. 1503–1509, 2022.

[21] I. H. Bell, J. Wronski, S. Quoilin, and V. Lemort, "Pure and pseudo-pure fluid thermophysical property evaluation and the open-source thermophysical property library coolprop," *Industrial and Engineering Chemistry Research*, vol. 53, no. 6, pp. 2498–2508, 2014.

[22] R. M. Tozer and R. W. James, "Fundamental thermodynamics of ideal absorption cycles," *International Journal of Refrigeration*, vol. 20, no. 2, pp. 120–135, 1997.

[23] H. Pieper, T. Ommen, B. Elmegaard, and W. Brix Markussen, "Assessment of a combination of three heat sources for heat pumps to supply district heating," *Energy*, vol. 176, pp. 156–170, 2019,

[24] V. Sharma, B. Shen, C. Keinath, M. Garrabrant, and P. Geoghegan, "European Regional Climate Zone Modeling of a Commercial Absorption Heat Pump Hot Water Heater," Proceedings from IEA Heat Pump Conference, 2017.

[25] "Inside the thermodynamic cycle." 2022. [Online]. Available: https://www.robur.com/en-us/media/inside-the-thermodynamic-cycle

[26] M. Garrabrant, R. Stout, C. Keinath, and P. Glanville, "Experimental Evaluation of Low-Cost Gas Heat Pump Prototypes for Building Space Heating," International Compressor Engineering, Refrigeration and Air Conditioning, and High Performance Buildings Conferences, 2016.

[27] C. M. Keinath, S. Garimella, and M. A. Garrabrant, "Modeling of an ammonia–water absorption heat pump water heater for residential applications," International Journal of Refrigeration, vol. 83, pp. 39–50, 2017.

[28] Canada Energy Regulator, "Market Snapshot: Decreasing GHG intensity of electricity generation reflects changes within the power sector." Accessed: December 29, 2024. [Online]. Available: https://www.cer-rec.gc.ca/en/data-analysis/energy-markets/market-snapshots/2016/market-snapshot-decreasing-ghg-intensity-electricity-generation-reflects-changes-within-power-sector.html